

Improved Quantitative Assessment of Left Ventricular Volumes Using TGrE Approach After Application of Extracellular Contrast Agent at 3 Tesla

Ashraf Hamdan,¹ Sebastian Kelle,¹ Bernhard Schnackenburg,² Eckart Fleck,¹ and Eike Nagel¹

Department of Internal Medicine/Cardiology, German Heart Institute Berlin, Berlin, Germany,¹
Philips Clinical Science, Hamburg, Germany²

ABSTRACT

Purpose: To prospectively determine whether the use of an extracellular contrast agent could improve the image quality of TGrE sequence for evaluation of left ventricular (LV) volumes and function, using a 3.0 T cardiovascular magnetic resonance (CMR) system. **Methods:** Fifteen consecutive patients underwent CMR imaging at 3.0 T. In each patient, 3 long axis views and multiple short axis slices with complete coverage of the left ventricle were performed using turbo gradient echo (TGrE) sequence before and after application of contrast agent 0.15 mmol/kg gadopentetate dimeglumine. LV volumes and ejection fractions were calculated using Simpson's rule and Area-Length-Method. For comparison of native and postcontrast TGrE, image quality, blood-to-myocardium contrast, and cardiac function parameters were assessed. **Results:** Application of contrast agent improves the image quality and blood-to-myocardium contrast in long-axis views. In short axis views, however, administration of contrast agent decrease the image quality and blood-to-myocardium contrast. After application of contrast agent in long axis scans, end-diastolic and end-systolic volumes were significantly larger (+ 12.9 mL [9%], $p < 0.02$; + 16.9 mL [17%], $p < 0.004$ respectively), and LV ejection fraction borderline lower (-4.1% [7%], $p = 0.08$). In short axis scans, however, end-diastolic and end-systolic volumes were significantly smaller (-14.8 mL [13%], $p < 0.001$; -17.6 mL [21%], $p < 0.004$ respectively), and LV ejection fraction borderline higher (3% [6%], $p = 0.052$). **Conclusion:** The use of an extracellular contrast agent improves the image quality for the assessment of LV volumes at 3.0 Tesla for TGrE sequence in long axis but not in short axis views.

INTRODUCTION

Cardiac function parameters such as left ventricular (LV) volumes and left ventricular ejection fraction (LVEF) are important prognostic factors in the diagnosis of patients suffering from ischemic heart disease (1). The accurate determination of functional parameters is crucial in deciding adequate therapeutic

strategies. Cardiovascular magnetic resonance (CMR) allows for multiplanar imaging with high intrinsic contrast and high temporal and spatial resolution. In addition, it has been shown to be highly accurate and reproducible (2), and, therefore, recognized as the standard of reference for the assessment of LV volumes and function (3).

At 1.5 T, the cine techniques based on balanced steady-state free precession (SSFP) sequences are the current standard for global functional analysis and regional wall motion. They generated an intrinsic high contrast between the myocardium and the ventricular blood-pool leading to an accurate and robust delineation of endo- and epicardial borders (4, 5). Turbo gradient echo (TGrE) cine, although equally accurate as the SSFP sequence (6), has lost its attraction for cardiac cine imaging. The disadvantage of TGrE cine is the lower contrast between blood-pool and myocardium. Especially in the long axis planes and in patients with impaired LV function, the image quality is limited by reduced signal intensity due to saturation of blood flowing predominantly in plane, which may hinder LV endocardial border delineation and, therefore, functional assessment (4).

Received 26 April 2007; accepted 9 August 2007

Keywords: Cardiovascular Magnetic Resonance, Left Ventricular Function, 3 Tesla, Contrast Agent.

Address correspondence to:

Dr Eike Nagel

Department of Internal Medicine/Cardiology

German Heart Institute Berlin

Augustenburger Platz 1, 13353 Berlin

Germany.

tel: +493045026280

fax: +493045026281

email: eike.nagel@dhzb.de

3.0 Tesla imaging systems are increasingly used in cardiac imaging (7, 8). There are, however, technical challenges for CMR imaging at 3 Tesla, particularly in relation to SSFP methods, due to their high sensitivity to off-resonance artefacts (7). In addition, TGrE sequences suffer in long axis from low contrast between blood-pool and myocardium due to inflow of saturated blood (7). These factors combined may make the assessment of LV function and volumes less accurate at 3.0 Tesla, both with TGrE and SSFP sequences. The use of contrast agents may provide an alternative approach for cardiac imaging independent of SSFP. If the T1 of the blood is short, then TGrE cine imaging with a very short repetition time becomes practical, with performance characteristics similar to those of SSFP. This may allow for the use of TGrE for wall motion imaging on 3.0 Tesla.

The use of extracellular contrast agents in combination with TGrE imaging was predominantly performed at 1.5 T, yielding improved contrast between blood and myocardium and, therefore, improved accuracy and reproducibility for evaluating LV volume and LVEF (9, 11). Therefore, the aim of our study was to evaluate the feasibility of cardiac cine MR imaging using native and postcontrast TGrE scans at 3.0 T, based on the comparison of image quality, blood-to-myocardium-contrast and global cardiac function parameters.

METHODS

Study population

Fifteen consecutive patients (range, 36–69 years, mean age 58 ± 9 years, 9 men, 6 women) with suspected (7 patients) or known coronary artery disease (8 patients) were enrolled into the study. Patients were excluded, if they had contraindications for CMR examinations such as noncompatible implants, claustrophobia, or arrhythmia such as atrial fibrillation or flutter. The study was conducted according the standards of the Charité institutional review board, and written informed consent was obtained by all patients.

Magnetic resonance imaging

CMR imaging was performed with the patient in the supine position by using a 3.0 Tesla whole body CMR scanner (Achieva 3.0 Tesla; Philips, Best, the Netherlands), equipped with a Quasar Dual gradient system (80 mT/m, 200 T/m/s slew rate). A six-element cardiac synergy coil was used for signal reception. All images were acquired in expiratory breath-holds. Cardiac synchronization was performed with vector electrocardiography and scans were triggered on the R-wave of the ECG (12). A rapid gradient echosequence (Multistack, multislice survey, TGrE, TR/TE/flip angle = 3.6 ms/1.7 ms/20°) allowed for localization of the heart in the three standard planes (transversal, coronal, and sagittal).

Standard TGrE imaging

The following standardized protocol was applied: rapid multislice survey; single-angulated, single-slice cine acquisition of

the LV; double angulated, single-section cine acquisition of the LV planned perpendicular to the previous view; contiguous short axis views covering the whole LV; 3 long axis views of the LV (two- three and four-chamber) planned on the short-axis orientation; application of 0.15 mmol gadobenate dimeglumine (MultiHance ALTANA, Bracco, Milan) pro kilogram of body weight; contiguous short axis views covering the whole LV with slice positions identical to the precontrast short axis images; and 3 long axis views of the LV (two- three and four-chamber) planned on the short-axis orientation with slice positions identical to the precontrast long axis images. The time period for planning and acquisition of the precontrast short axis views was 656 ± 77 s.

Parameters of the native and postcontrast cine TGrE sequences were as follows: TR/TE/ flip angle = 4 ms/2.5 ms/15°; 30 phases/cardiac cycle; in plane spatial resolution = 2×2 mm with a slice thickness of 8 mm.

Image analysis

Visual assessment

Image quality of each standard view (long and short axis) was graded on a four-point scale. The visual score refers to the visibility of the endocardial border (score 1: poor or nondiagnostic; 2: moderately or partly visible; score 3: well visible; and 4: excellently visible).

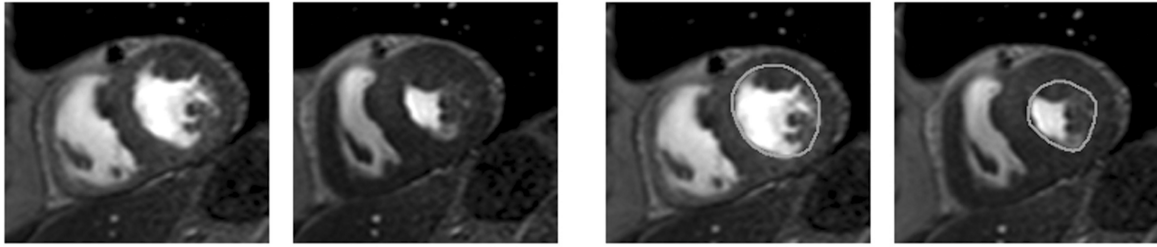
Signal intensity measurements

For native and postcontrast TGrE cine imaging, mean signal intensity (SI) of the myocardium and blood-pool was measured at end-diastole in long and short axis views. For long axis images, the region of interest (ROI) was placed in the mid septal myocardium of a four chamber view in end-diastole and the mean SI was determined. The SI of the blood was defined as the mean signal from a circular ROI drawn in the center of the left ventricle at end-diastole sparing the papillary muscles. For short axis images the corresponding equatorial slice was used to define the SI of the myocardium and blood in the same way as for the four chamber view. The contrast between blood and myocardium was calculated as: Contrast = $SI_{\text{blood}} / SI_{\text{Myocardium}}$.

LV parameters

The data was transmitted to an offline image processing station (ViewForum Release 4, Philips Medical System) for analysis of both native and postcontrast TGrE cine imaging. For volume measurements, endocardial borders were traced manually at end-diastole and end-systole in the short axis projection (Fig. 1) with papillary muscles excluded from the analysis; the most basal section of the left ventricle was defined for end-diastole and end-systole as the slice at which at least 50% of the LV myocardial circumference was visible. The volumes were calculated as the sum of the areas of the LV cavity multiplied by slice thickness. LV end-diastolic volume (LVEDV) and LV end-systolic volume (LVESV) were assessed by applying Simpson's rule and LVSV and LVEF was calculated.

TGrE without CA



TGrE with CA

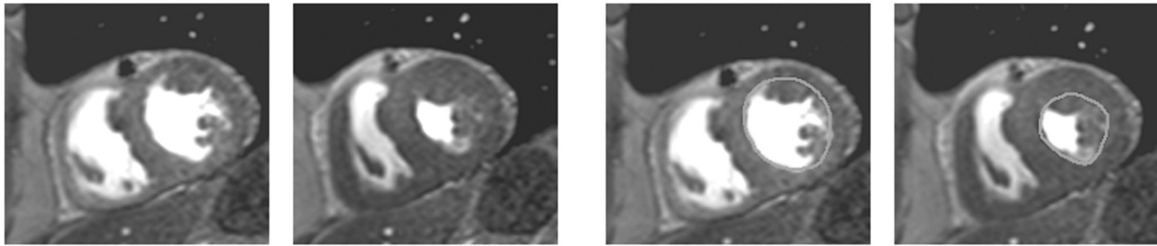
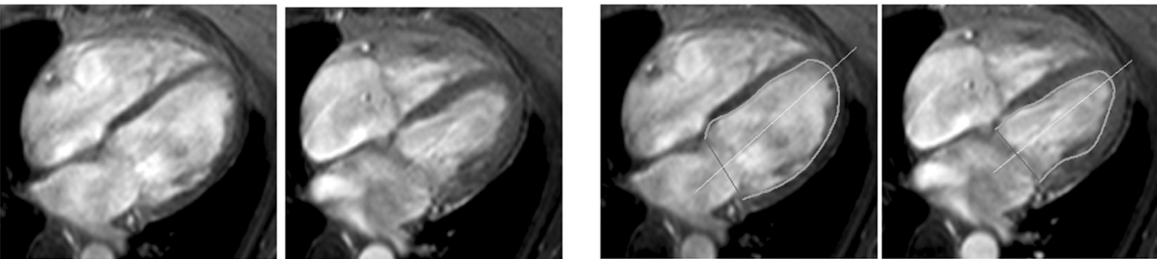


Figure 1. Representative example of endocardial contour delineation in short axis. Identical short-axis geometry acquired with precontrast (upper row) and postcontrast (bottom row) cine imaging is given. LV endocardial contours were traced manually at end-diastole (left) and end-systole (right) to calculate LV volumes and LVEF according to Simpson's rule.

TGrE with CA



TGrE without CA

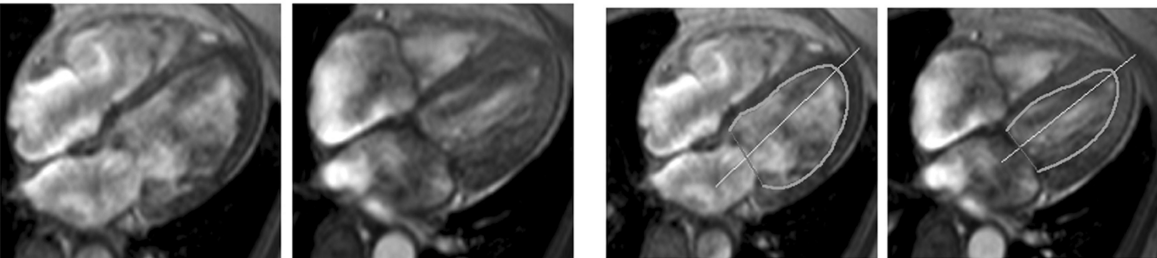
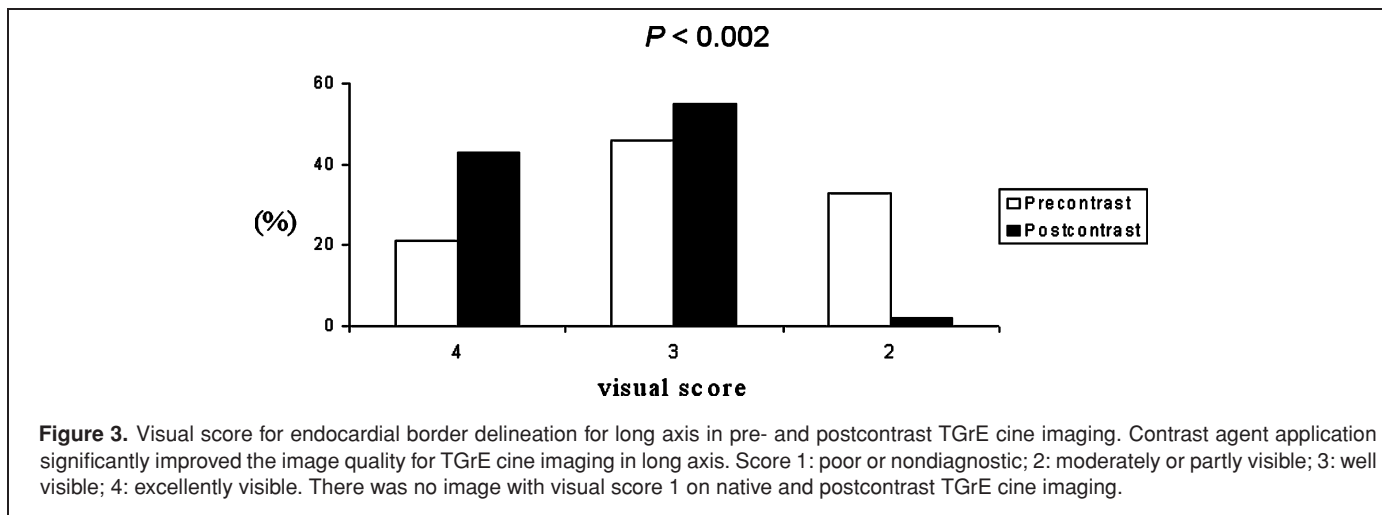


Figure 2. Representative example of endocardial contour delineation in long axis. Identical four chamber view geometry acquired with postcontrast (upper row) and pretcontrast (bottom row) cine imaging is given. LV endocardial contours were traced manually at end-diastole (left) and end-systole (right) to calculate LV volumes and LV ejection fraction according to Area-Length Method. The image quality and endocardial contour delineation suffers from saturation effects before contrast agent administration.



In addition, LV volumes were obtained in the long-axis projections. Using the four chamber view, LV endocardial borders were traced at end-diastole and end-systole and the papillary muscles were excluded from the analysis. LV end-diastolic and end-systolic cross sectional area and the ventricular length, measured from the mitral valve annulus to the endocardial border of the apex, were measured (Fig. 2). LVEDV and LVESV were assessed according to area-length method (LV volume = $0.85 \times \text{LV-area}^2 / \text{LV-length}$) and LVSV and LVEF were calculated.

Statistical analysis

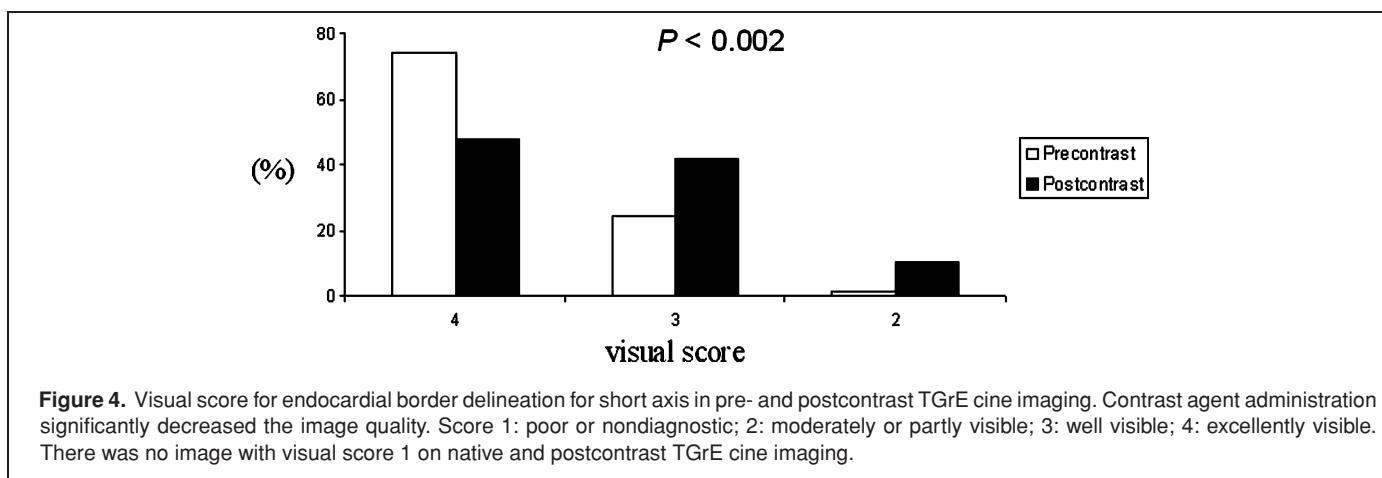
Statistical analysis was performed by using a statistical software package (SPSS, Chicago, Illinois, USA). For all continuous parameters, data is given as mean \pm standard deviation. All tests were two-tailed, and a $p < 0.05$ was considered to indicate a statistical significant difference. The paired Student t test was used to assess statistical significance of continuous variables. Wilcoxon Signed ranks test was used to evaluate the statistical significant between the visual score of pre- and postcontrast TGrE. Bland-Altman analysis was performed to compare the

two imaging techniques with regard to LV volumes and ejection fraction, the degree of agreement between these two methods were determined as mean absolute difference, 95% confidence intervals of the mean difference, and mean relative difference (the mean of the two modalities divided by their mean value) (13).

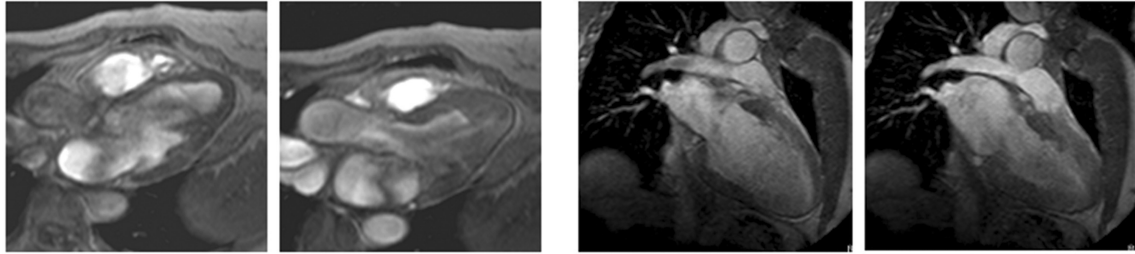
RESULTS

Visual score

All examination on both native and postcontrast TGrE cine imaging yielded diagnostic image quality (i.e., visual score ≥ 2). Application of contrast agent significantly improved the image quality for TGrE cine imaging in long axis ($p < 0.002$) (Fig. 3). In short axis views, however, administration of contrast agent significantly decreased the image quality ($p < 0.002$) (Fig. 4). The endocardial contours delineation differed most around papillary muscles and trabeculations at end-diastolic and end-systolic imaging. In long axis views, application of contrast improves endocardial border delineation (Figs. 2 and 5). In short axis views, however, delineation of endocardial contours



TGrE without CA



TGrE with CA

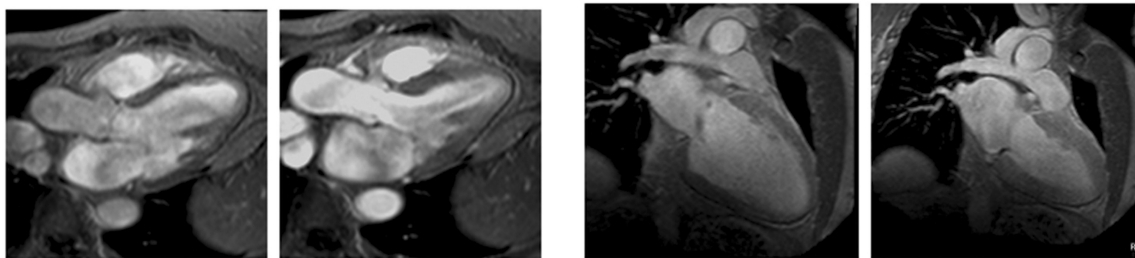


Figure 5. Long axis views of the left ventricle with native (upper row) and postcontrast (bottom row) TGrE cine imaging. Three chamber view (left) and two chamber view (right) at end-diastolic (right) and end-systolic (left) frames. The image quality and endocardial contour delineation suffers from saturation effects before contrast agent application.

was easier in native images compared to postcontrast images (Figs. 1 and 6).

Signal intensity

Blood-to-myocardium-contrast (BMC) for native and post-contrast TGrE cine imaging in long and short axis views is shown in Table 1. After application of contrast agent, the SI measurements showed an increase in the BMC of 38% from 1.58 to 2.18 in the long axis views. In the short axis views; however, the BMC decreased by 50% from 3.4 to 1.7.

LV parameters

Table 2 shows the differences between native and postcontrast TGrE measurements for LV cardiac parameters in long and short axis views. After application of contrast agent in long axis scans, end-diastolic and end-systolic volumes were significantly larger (+ 12.9 mL [9%], $p < 0.02$; + 16.9 mL [17%], $p < 0.004$, respectively) and LVEF borderline lower (-4.1% [7%], $p = 0.08$). In short axis scans, however, end-diastolic and end-systolic volumes were significantly smaller (-14.8 mL [13%], $p < 0.001$; -17.6 mL [21%], $p < 0.004$, respectively) and LVEF borderline higher (3% [6%], $p = 0.052$) (Table 2, Fig. 7).

Precontrast TGrE scans in short axis views, which have the highest visual score and BMC, showed agreement with post-

contrast but not with native TGrE in long axis view (Table 3, Fig. 8).

DISCUSSION

With the use of an extracellular contrast agent, it was possible to achieve higher image quality with less blood flow dependence and greater blood-to-myocardium contrast at the endocardial border in long axis scans. The results of contrast agent application using the same sequence reflect an opposite change of image quality and blood-to-myocardium contrast for short axis scans at 3.0 T. Contrast agent application might, therefore, have quantitative advantages in long axis views. Our data demonstrate, after application of contrast agent, LV end-diastolic and end-systolic volumes were larger in long axis and smaller in short axis.

In the current study, both the image quality and blood-to-myocardium contrast in postcontrast long axis and precontrast short axis were higher compared with that of precontrast long axis and postcontrast short axis images. Because Simpson's method is the reference standard for assessment of LV volumes (3), we used precontrast short axis images as the reference method in this study. No differences in measured parameters using precontrast short axis and postcontrast long axis were found (Table 3A, Fig. 8). In contrast, the differences between LV parameters using precontrast short axis and precontrast long

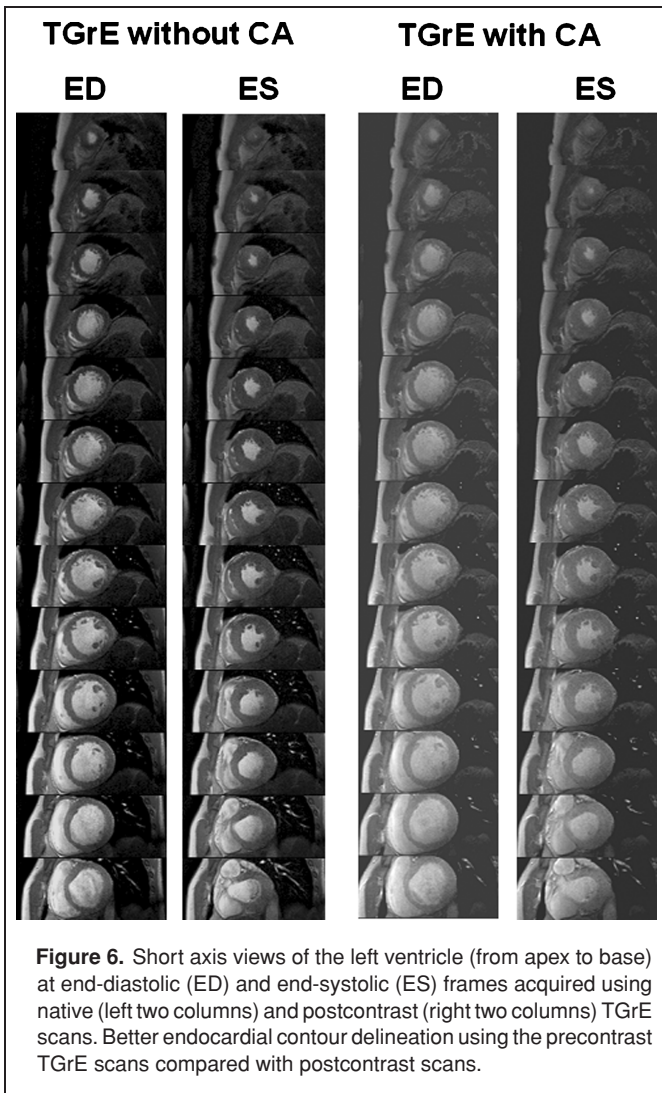


Figure 6. Short axis views of the left ventricle (from apex to base) at end-diastolic (ED) and end-systolic (ES) frames acquired using native (left two columns) and postcontrast (right two columns) TGrE scans. Better endocardial contour delineation using the precontrast TGrE scans compared with postcontrast scans.

axis were significant (Table 3B, Fig. 8). Therefore, postcontrast TGrE scans in long axis and native TGrE scans in short axis resulted in a similar and reproducible LV volumes and ejection fractions.

From the data presented here, volumetric differences arise for different endocardial contour drawing. The endocardial contour was drawn larger in postcontrast long axis views, the surface slow-flow boundary layer around papillary muscles and trabeculations on precontrast long axis images can make papillary muscles appear larger and confluent with myocardium and can make blood between trabeculations appear as myocardium. An equivalent effect can be found if LV mass is assessed in systole, when trabeculae are more confluent (14). The importance

Table 1. Blood-To-Myocardium-Contrast for post- and precontrast TGrE scans in long and short axis view

	Postcontrast TGrE	Precontrast TGrE	P value
Long axis	2.18 ± 0.3	1.58 ± 0.2	<0.001
Short axis	1.7 ± 0.1	3.4 ± 0.9	<0.001

Table 2. Cardiac function parameters acquired using post- and precontrast TGrE scans in long axis views (Area-Length-Method) and short axis views (Simpson's rule)

	Postcontrast TGrE	Precontrast TGrE	Absolute Difference	Percentage Difference	P-value
Long axis					
LVEDV (ml)	170 ± 66	158 ± 71	12.9 ml	9	0.02
LVESV (ml)	85 ± 53	68 ± 36	16.9 ml	17	0.004
LVEF (%)	53 ± 12	57 ± 8	-4.1	-7	0.08
Short axis					
LVEDV (ml)	153 ± 74	168 ± 76	-14.8 ml	-13	0.001
LVESV (ml)	70 ± 42.6	86 ± 55	-17.6 ml	-21	0.004
LVEF (%)	56 ± 7.2	51 ± 11	3%	6	0.052

of trabeculae and papillary muscles for LV parameters has been previously commented on (15). In addition the low blood-to-myocardium contrast on native long axis, images makes the delineation between blood and myocardium difficult. In native short axis views, the blood-to-myocardium contrast was higher and, therefore, the endocardial border delineation was more accurate compared with that using postcontrast short axis images.

CMR in native short axis yields images with high contrast between blood-pool and myocardium because of the dominant through-plane blood flow, which resulted, in improved image quality and blood-to-myocardium contrast of native short axis images in comparison to postcontrast short axis images. Problems occur, however, with long axis images because of saturation of blood, which flows predominantly in plane and is subject to repeated excitations. This saturation effect is even more pronounced at 3 Tesla versus 1.5 Tesla due to the longer T1 values. Therefore, application of T1 shortening contrast agent significantly improved image quality and blood-to-myocardium contrast of long axis images.

Currently, initial reports suggest the feasibility of delayed enhanced CMR and first-pass myocardial perfusion imaging at 3.0 T (10, 16). In addition, it has been shown that functional cardiac cine CMR imaging may be regarded as equally accurate at 3.0 T compared with 1.5 T (7). However, the question arises which approach is the most gainful to take advantage from the introduction of high-field CMR imaging. Unlike TGrE, SSFP is relatively insensitive to flow but shows a higher sensitivity to off resonance artefacts. In one study comparing SSFP with TGrE at 3.0 T, 85% of all SSFP examinations at high field strengths exhibited severe off-resonance artifacts and the signal to noise ratio gain was higher for TGrE (7). Therefore, TGrE sequence seems to be much more convenient for 3.0 T.

LIMITATION

An unresolved question of the study is which measurement technique is more accurate. The image quality and higher blood-to-myocardium contrast of postcontrast TGrE in long axis and native TGrE scans in short axis leads to the assumption that endocardial border delineation and therefore LV volumes

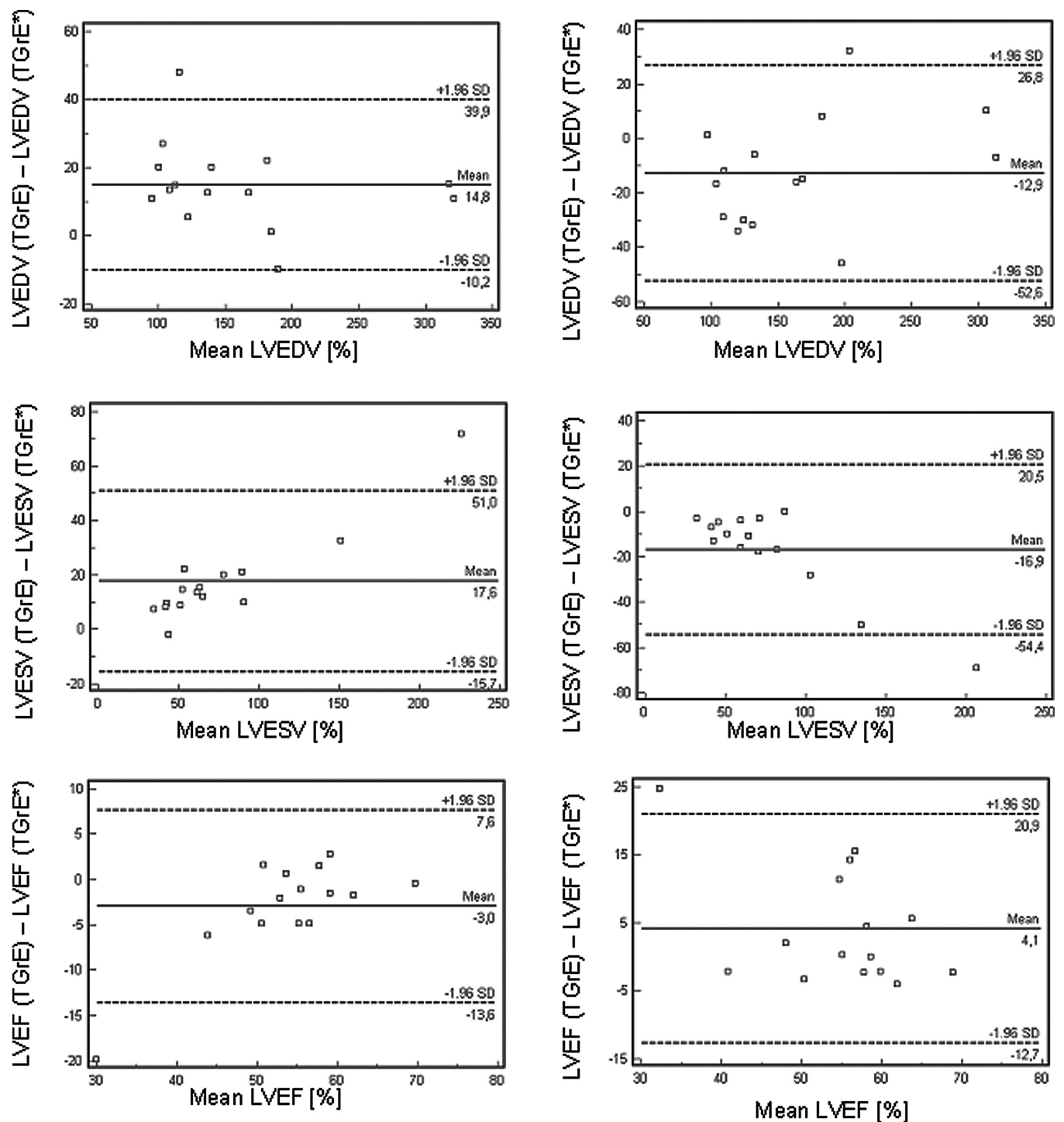


Figure 7. Bland-Altman plots of left ventricular parameters in short (left column) and long (right column) axis views demonstrating: disagreement between native and postcontrast TGrE scan for LV end-diastolic volume (LVEDV) and LV end-systolic volume (LVESV) and agreement between both methods for assessment of LV ejection fraction (LVEF). For native and postcontrast cine imaging, the differences (within mean \pm 1.96 standard deviations) for LVEDV and LVESV were clinically relevant. In contrast, the differences for LVEF were not clinically relevant. In each plot, the central line indicates the mean absolute difference, and upper and lower lines represent 95% CIs. TGrE* indicates TGrE after application of contrast agent.

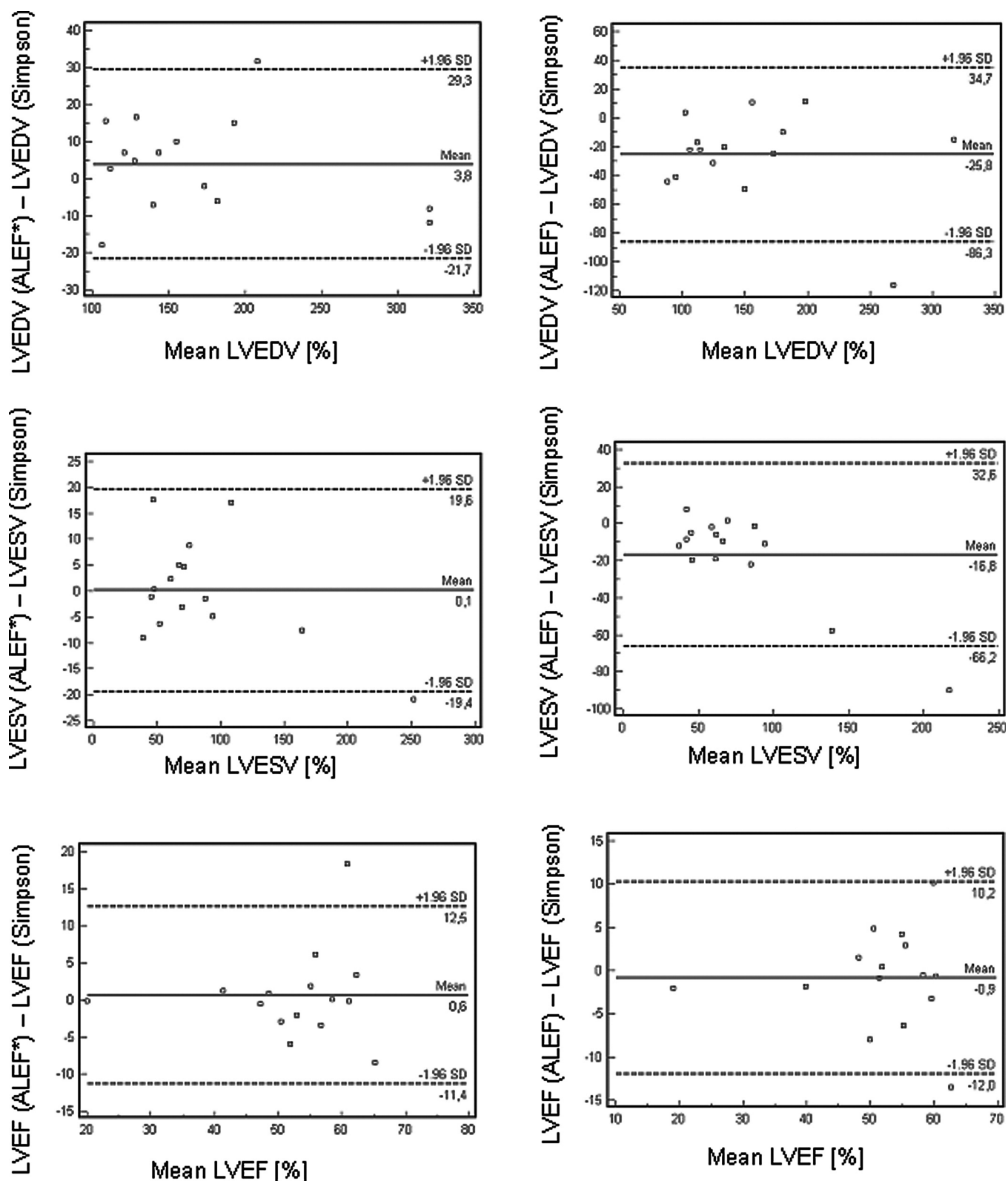


Figure 8. Bland-Altman plots illustrating agreement between postcontrast TGrE scans in long axis and native TGrE scans in short axis for LVEDV, LVESV, and LVEF (left column) and clinically relevant differences between precontrast TGrE scans in long axis and native TGrE scans in short axis for LVEDV and LVESV, the differences for LVEF were clinically not significant (right column). According to the visual score and Blood-To-Myocardium-Contrast, native TGrE cine imaging in short axis (Simpson's method) is the reference standard for assessment of LV volumes and ejection fraction. TGrE* indicates TGrE after application of contrast agent.

Table 3. Cardiac function parameters acquired using precontrast TGrE scans in short axis views in comparison with postcontrast TGrE scans in long axis views (A) and precontrast TGrE scans in long axis views (B)

A					
	Precontrast TGrE (short axis)	Postcontrast TGrE (long axis)	Absolute Difference	Percentage Difference	<i>P</i> - <i>value</i>
LVEDV	168 ± 76	170 ± 66	-3.8 ml	-3.5	0.4
LVESV	86 ± 55	85 ± 53	-2.4 ml	-2.4	0.9
LVEF	51 ± 11	53 ± 12	-0.6 %	-1.4	0.7
B					
	(short axis)	(long axis)	Difference	Difference	<i>value</i>
LVEDV	168 ± 76	158 ± 71	12.9 ml	6.6	0.02
LVESV	86 ± 55	68 ± 36	16.8 ml	14.9	0.02
LVEF	51 ± 11	57 ± 8	0.9%	1.4	0.06

measurements is more accurate using precontrast short axis and postcontrast long axis cine imaging.

Phantom studies could be used to calibrate our measurements techniques; however, pre- and postcontrast differences in long axis imaging are likely to be flow related, which occur at complex blood-myocardium interfaces. Differentiating these complex issues would sophisticate phantoms and substantial extrapolation to the in vivo situation. Another possibility may be to calibrate our measurements against explanted human hearts, but in practice these studies are difficult to perform, the time between imaging and transplantation unpredictable and often long, and it cannot be assumed that the heart remains the same during this interval. Thus, the ventricular volumes are unlikely to be calibrated to the accuracy required.

CONCLUSION

The application of extracellular contrast agent improved image quality and blood-to-myocardium contrast in long axis views, leading to a better endocardial border delineation and, therefore, to a larger LV volumes as compared with native long axis cine imaging. In contrast, application of contrast agent decreased both image quality and blood-to-myocardium contrast of short axis cine. Therefore at 3.0 T, we suggest the following rapid “one-stop shop” integrated CMR imaging protocol: short axis cine imaging before contrast agent administration and long axis cine imaging after application of MultiHance for first pass perfusion imaging. Finally, late enhancement imaging can be performed after a waiting period of 5–10 minutes after the application of contrast agent.

REFERENCES

1. Sanz G, Castaner A, Betriu A, Magrina J, Roig E, Coll S, Pare JC, Navarro-Lopez F. Determinants of prognosis in survivors of myocardial infarction: a prospective clinical angiographic study. *N Engl J Med* 1982;306:1065–1070.

2. Pattynama PM, Lamb HJ, van der Velde EA, van der Wall EE, de Roos A. Left ventricular measurements with cine and spin-echo MR imaging: a study of reproducibility with variance component analysis. *Radiology* 1993;187(1):261–8.
3. Pennell DJ, Sechtem UP, Higgins CB, Manning WJ, Pohost GM, Rademakers FE, van Rossum AC, Shaw LJ, Yucel EK. Clinical indications for cardiovascular magnetic resonance (CMR): Consensus Panel report. *Eur Heart J* 2004;25(21):1940–1965.
4. Barkhausen J, Ruehm SG, Goyen M, Buck T, Laub G, Debatin JF MR evaluation of ventricular function: true fast imaging with steady-state precession versus fast low-angle shot cine MR imaging: feasibility study. *Radiology* 2001;219:264–269.
5. Moon JC, Lorenz CH, Francis JM, Smith GC, Pennell DJ. Breath-hold FLASH and FISP cardiovascular MR imaging: left ventricular volume differences and reproducibility. *Radiology* 2002;223:789–797.
6. Michaely HJ, Nael K, Schoenberg SO, Laub G, Reiser MF, Finn JP, Ruehm SG. Analysis of cardiac function—comparison between 1.5 Tesla and 3.0 Tesla cardiac cine magnetic resonance imaging: preliminary experience. *Invest Radiol* 2006;41(2):133–140.
7. Wintersperger BJ, Bauner K, Reeder SB, Friedrich D, Dietrich O, Sprung KC, Picciolo M, Nikolaou K, Reiser MF, Schoenberg SO. Cardiac steady-state free precession CINE magnetic resonance imaging at 3.0 tesla: impact of parallel imaging acceleration on volumetric accuracy and signal parameters. *Invest Radiol* 2006;41(2):141–147.
8. Thiele H, Nagel E, Paetsch I, Schnackenburg B, Bornstedt A, Kouwenhoven M, Wahl A, Schuler G, Fleck E. Functional cardiac MR imaging with steady-state free precession (SSFP) significantly improves endocardial border delineation without contrast agents. *J Magn Reson Imaging* 2001;14(4):362–367.
9. Pennell DJ, Underwood SR, Longmore DB. Improved cine MR imaging of left ventricular wall motion with gadopentetate dimeglumine. *J Magn Reson Imaging* 1993;3(1):13–19.
10. Klumpp B, Fenchel M, Hoewelborn T, Helber U, Scheule A, Claussen C, Miller S. Assessment of myocardial viability using delayed enhancement magnetic resonance imaging at 3.0 Tesla. *Invest Radiol* 2006;41(9):661–667.
11. Matsumura K, Nakase E, Haiyama T, Takeo K, Shimizu K, Yamasaki K, Kohno K. Determination of cardiac ejection fraction and left ventricular volume: contrast-enhanced ultrafast cine MR imaging vs IV digital subtraction ventriculography. *AJR Am J Roentgenol* 1993 May;160(5):979–985.
12. Fischer SE, Wickline SA, Lorenz CH. Novel real-time R-wave detection algorithm based on the vectorcardiogram for accurate gated magnetic resonance acquisitions. *Magn Reson Med* 1999;42:361–370.
13. Bland JM, Altman DG. Statistical methods for assessing agreement between two methods of clinical measurement. *Lancet* 1986;1(8476):307–310.
14. Marcus JT, Kuijper JPA, Gotte RM. Left ventricular mass measured by magnetic resonance imaging: effect of endocardial trabeculae on the observed wall thickness (abstr). *J Cardiovasc Magn Reson* 2000; 2:301–302.
15. Ibrahim T, Weniger M, Schwaiger M. Effect of papillary muscles and trabeculae on left ventricular parameters in cine-magnetic resonance images (MRI) (abstr). *J Cardiovasc Magn Reson* 1999;1:319.
16. Araoz PA, Glockner JF, McGee KP, Potter DD Jr, Valeti VU, Stanley DW, Christian TF. 3 Tesla MR imaging provides improved contrast in first-pass myocardial perfusion imaging over a range of gadolinium doses. *J Cardiovasc Magn Reson* 2005;7(3):559–564.